First-principles calculation of the interaction energy of $((3)^{1/2}\times(3)^{1/2})$ R 30° Xe/Pt(111)

2000 J. Phys.: Condens. Matter 12 7077

(http://iopscience.iop.org/0953-8984/12/31/309)

J. Phys.: Condens. Matter **12** (2000) 7077–7088. Printed in the UK PII: S0953-8984(00)12038-7

First-principles calculation of the interaction energy of $(\sqrt{3} \times \sqrt{3})$R30° Xe/Pt(111)

A E Betancourt and D M Bird
Department of Physics, University of Bath, Bath BA2 7AY, UK

Received 21 February 2000, in final form 13 June 2000

Abstract. Calculations of the energy of the interaction between Xe and Pt(111) in the $(\sqrt{3} \times \sqrt{3})$R30° structure are reported. A density functional approach is used with a slab geometry and a pseudopotential formalism. Exchange–correlation effects are treated within the local density approximation and the generalized gradient approximation. The local density approximation gives a well depth comparable to that obtained from experiment whereas the generalized gradient approximation gives very weak binding. Both approximations predict that the on-top site is the most favourable position for the adsorption of Xe atoms. The binding mechanism is discussed in terms of the charge density and the local density of states.

1. Introduction

As a result of the development of rare-gas scattering as a technique for studying the structural characteristics of clean and adsorbate-covered surfaces there has been considerable recent interest in understanding the interaction between rare-gas atoms and crystalline surfaces (for a recent review see [1]). The interaction potential energy is the fundamental quantity which is needed to provide an accurate interpretation of diffraction measurements and, for this reason, it is important to construct potentials which accurately reflect the details of the atom–surface interaction.

Usually, the interaction potential is constructed from empirical models which are fitted to reproduce a variety of experimental quantities. There have been relatively few attempts to calculate the potential in a direct manner, especially using first-principles calculations. One problem here is that it is not clear how to model the rare-gas–surface interaction within density functional theory (DFT). It is now established that *chemical* binding energies calculated with the local density approximation (LDA) for exchange and correlation have been improved systematically by using the generalized gradient approximation (GGA) (see [2–6], and references therein). However, for systems with weak interactions the improvement of the GGA over the LDA is not so clear. For example, for rare-gas diatomics with He or Ne atoms, the GGA reduces the overbinding of the LDA, but for diatomic molecules with heavier rare-gas atoms the GGA predicts a very weak binding energy [7, 8]. In the context of rare-gas/surface systems, recent calculations using all-electron DFT schemes have reported a good agreement with experiment for He/Rh(110) and Ne/Rh(110) using the GGA [9] and for He/Ag and Ne/Ag using the LDA [10]. An alternative approach has been the development of new functionals which explicitly include the van der Waals interaction within the formalism of DFT (see, for example, [11] and references therein). Recent progress in this area has been encouraging, but applications to date have been limited to relatively simple systems.

0953-8984/00/317077+12$30.00

The interaction of Xe atoms with metallic surfaces, and in particular with Pt(111), has been widely studied both theoretically and experimentally [12–17] and therefore provides a good test of different theoretical approaches. In particular, for Xe/Pt(111), Barker and Rettner [16] have constructed an empirical potential which is consistent with a wide range of dynamical and equilibrium experimental data. This potential has been used by several groups to study the dynamics of rare-gas/surface systems [18–20]. In this paper, we therefore use Barker and Rettner's potential as a benchmark for testing the accuracy of LDA and GGA potentials. The first non-empirical calculation for Xe/Pt(111) was carried out by Müller [14] using the LDA and a cluster to represent the Pt surface. Our aim is to extend this work to a comparison of LDA and GGA potentials for one of the experimentally observed phases for Xe/Pt(111), namely the commensurate $(\sqrt{3} \times \sqrt{3})$R30° structure [13]. To do this we use a first-principles pseudopotential approach, with the surface modelled using a slab/supercell geometry. In section 2 details of the calculations are described and in section 3 results for the LDA and GGA potentials are given, together with a comparison with experiment and with the Barker–Rettner potential. Section 4 presents an analysis of the electronic structure of the Xe/Pt system.

2. Computational details

The interaction potential is obtained from DFT total-energy calculations using a mixed-basis approach [21]. Here, the Kohn–Sham wave function is expanded in a basis set which consists of pseudo-atomic orbitals and low-energy plane waves:

$$\psi_{\alpha \boldsymbol{k}}(\boldsymbol{r}) = \sum_{\mu} a_{\mu}^{\alpha}(\boldsymbol{k}) \chi_{\mu}(\boldsymbol{r}) + \frac{1}{\sqrt{\Omega}} \sum_{\boldsymbol{G}} a_{\boldsymbol{G}}^{\alpha} \exp(\mathrm{i}(\boldsymbol{k} + \boldsymbol{G}) \cdot \boldsymbol{r}) \tag{1}$$

which together are suitable for describing both the localized and delocalized character of the electronic wave function. In equation (1), α is the band index, μ is a combined index which labels the orbitals and atomic sites, a_{μ} and $a_{\boldsymbol{G}}$ are coefficients of the pseudo-atomic orbitals and plane waves, respectively, and Ω is the volume of the unit cell. χ_{μ} is the Bloch sum formed from pseudo-atomic orbitals as

$$\chi_{\mu}(\boldsymbol{r}) \equiv \chi_{m}^{i}(\boldsymbol{r}) = \sum_{\boldsymbol{R}_l} \exp(\mathrm{i}\boldsymbol{k} \cdot (\boldsymbol{R}_l + \boldsymbol{\tau}_i)) \phi_m(\boldsymbol{r} - \boldsymbol{R}_l - \boldsymbol{\tau}_i) \tag{2}$$

where m labels the orbitals, the $\boldsymbol{R}_l$ are lattice vectors, the $\boldsymbol{\tau}_i$ are atomic coordinates and the ϕ_m are pseudo-atomic orbitals. A momentum-space approach is adopted which allows the rapid evaluation of matrix elements, and the maximum number of reciprocal-lattice vectors which contribute is defined in terms of a cut-off energy. This is the main parameter that controls the convergence of the total energy and is identical to the plane-wave cut-off energy used in a standard plane-wave calculation [21]. Our calculated potentials have been tested against full plane-wave calculations with the same cut-off energy and in all cases the results differ by less than 5 meV. The advantage of using the mixed-basis approach is an increase in speed by a factor of about four, together with the ease in performing an orbital-based decomposition of the electronic structure. Using the mixed orbital/plane-wave basis the Kohn–Sham equations are solved by direct diagonalization. Self-consistency in the charge density is achieved by using a combination of Kerker mixing [22] and a modified Broyden method [23]. Pre-conditioning [24] is used in order to minimize the number of iterations required for convergence.

Semi-relativistic, norm-conserving pseudopotentials were generated for Pt and Xe from fully relativistic all-electron calculations using Troullier and Martins' scheme [25] and are produced in the separable Kleinman–Bylander form [26]. For Pt, s and d potentials (and their

associated pseudo-atomic orbitals) were obtained from the ground configuration $6s^1 5d^9 6p^0$ and the p parts from the ionic configuration $6s^{0.25} 5d^8 6p^{0.75}$. In the case of Xe we used $5s^2 5p^6 5d^0$ for the s and p parts and $5s^1 5p^{4.75} 5d^{0.25}$ for the d part [27]. Because the accuracy of the calculated interaction energy is a key requirement for these calculations, more attention was paid to producing highly transferable pseudopotentials than to optimization in order to reduce the plane-wave cut-off energy. The pseudopotential core radii were therefore chosen to provide the best match between the logarithmic derivatives of pseudo-atoms and all-electron atoms over an energy range between −2.0 Ryd and 1.5 Ryd. The optimal core radii for Pt were 2.30, 2.75 and 2.30 for s, p and d states respectively; the equivalent values for Xe were 1.73, 1.90 and 3.80 (all values are in Bohr radii). The Ceperley–Alder parametrization of the LDA [28] and the form of the GGA given by Perdew, Burke and Ernzerhof (PBE) [29] were used for exchange–correlation effects. The PW91 form of the GGA [30] was also used, but gave very similar results to the GGA-PBE form. For both LDA and GGA potentials, non-linear core corrections (see [31] and references therein) were considered in order to improve the transferability of the pseudopotential.

The Pt and Xe pseudopotentials were tested for bulk Pt and the dimer Xe_2. Table 1 summarizes the calculated lattice constants and bulk moduli for Pt and the bond lengths and well depths for Xe_2. Cut-off energies of 500 eV for the expansion of the localized orbitals and 60 eV for the low-energy plane waves were used. In both cases, these provide a convergence of better than 0.01 Å in the interatomic distance. The Pt lattice constants in table 1 are close to the experimental values and to previous calculations, with the LDA providing the best agreement between theory and experiment. The bulk modulus shows more sensitivity to the form of the exchange–correction functional; the underestimation of the bulk modulus with the GGA-PBE form is a consequence of the overestimation the lattice constant. In the case of the Xe_2 dimer, the molecule was placed in a box of size $9 \times 9 \times 15$ Å^3 (large enough for intermolecular interactions to be negligible) and the distance between the Xe atoms was varied between 3 Å and 6 Å. The results show that there is a noticeable underestimation of the bond length and a large overestimation in the well depth with the LDA, which the GGA-PBE form overcorrects. Similar behaviour has been reported by Patton and Pederson for the binding energy in diatomic molecules that contain Ar and Kr [8]. Table 1 also shows that non-linear core corrections give a small effect with the LDA but with the GGA-PBE form they are more significant, tending to give a larger underestimate of the bulk modulus in Pt and larger overestimate of the bond length in Xe_2.

Table 1. The lattice constant, a_0, and bulk modulus, B, for fcc Pt and the bond length, r_e, and well depth, D_e, for Xe_2 obtained using the LDA and the GGA-PBE form with and without non-linear core corrections (NLCC). All-electron (AE) and experimental results also are shown.

	LDA	LDA–NLCC	PBE	PBE–NLCC	Experiment	AE-LDA	AE-PW91
a_0 (Å)	3.93	3.94	4.02	4.02	3.92[a]	3.89[a]/3.90[b]	3.97[a]/3.97[b]
B (GPa)	285	283	243	235	283[a]	306[a]/307[b]	263[a]/246[b]
r_e (Å)	3.98	3.99	4.66	4.77	4.3[c]		
D_e (meV)	43.6	43.8	7.6	8.9	23.4[c]		

[a] Reference [32].
[b] Reference [34].
[c] Reference [33].

The interaction potential energy was estimated by subtracting the total energy of the clean slab and of an Xe atom from the total energy of the slab with absorbed Xe. The (slab + Xe) and bare-slab energies were calculated in the same supercell and keeping all aspects of the

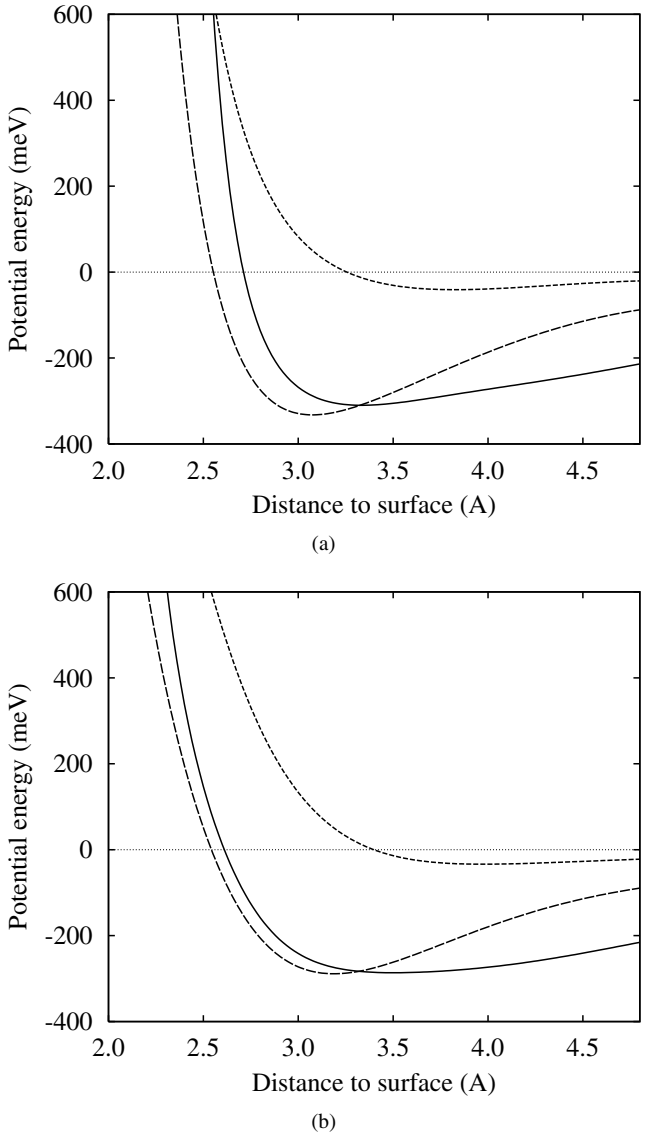

Figure 1. The interaction potential energy for $(\sqrt{3} \times \sqrt{3})$R30° Xe/Pt(111) as a function of height from the first surface layer; (a) at the on-top site, (b) at the fcc-hollow site, (c) at the bridge site. The Barker–Rettner, LDA and GGA-PBE potentials are shown by full, long-dashed and short-dashed lines respectively.

calculation the same. The energy of an isolated Xe atom was calculated in a (15 Å)^3 box with the same cut-off energies as for the slab calculations. Because the reference is taken to be an isolated Xe atom, our calculated potentials include the lateral interaction energy of a layer of Xe atoms in the $(\sqrt{3} \times \sqrt{3})$ structure. This energy is found to be -59 meV and -17 meV for the LDA and the GGA-PBE form respectively, where the minus sign indicates that the interaction is attractive. The equivalent value for the Barker–Rettner potential is -56 meV, and, on the basis of fits to thermal desorption data, Widdra *et al* [35] estimate a value of -33 meV. In order to guarantee a high level of precision, the convergence of the interaction potential was checked

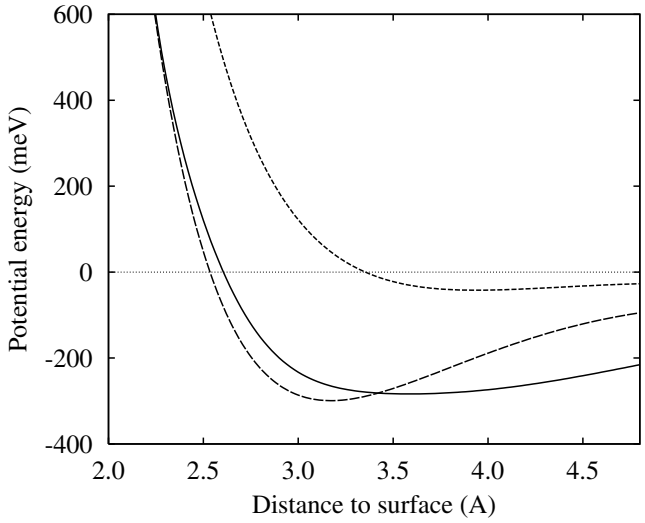

(c)

Figure 1. (Continued)

as a function of the cut-off energies, the number of special k-points, the number of Pt layers and the size of the vacuum gap. The final choice of parameters was as follows: 500 eV cut-off for the expansion of the pseudo-atomic orbitals in (2); 60 eV for the extra, low-energy plane waves in (1); the full surface Brillouin zone was sampled by 54 k-points; and the supercell contained five Pt layers and nine equivalent layers of vacuum, which is approximately 20 Å. Extensive tests show that these values provide a precision of order 5 meV in the interaction potential for the ($\sqrt{3} \times \sqrt{3}$)R30° Xe/Pt(111) system, taking as a reference calculations based on the LDA.

The mechanism of the binding between the adsorbate and substrate was studied by analysis of the density of electronic states projected onto the basis functions in equations (1) and (2). This quantity is defined by (see also [36, 37])

$$d^i(E) = \sum_{\alpha \boldsymbol{k}} \sum_j a_j^{\alpha *} S_{ji} a_i^{\alpha} \delta(E - E_{\alpha \boldsymbol{k}}) \tag{3}$$

where i and j label the basis functions in equation (1) (i.e. either a pseudo-atomic orbital μ, or a low-energy plane wave $\boldsymbol{G}$) and S_{ji} is the overlap matrix connecting basis functions. With this definition, the total density of states is exactly the sum of $d^i(E)$ over all basis states, and so the total charge associated with any basis function can be defined by

$$Q^i = \int_{-\infty}^{E_F} d^i(E)\, \mathrm{d}E \tag{4}$$

which is equivalent to the charge of the orbital i within Mulliken's analysis [38]. In practice, we are most interested in projections onto the pseudo-atomic orbitals but, within the mixed-basis approach, plane-wave parts are also present. It is found that the integrated charges defined by equation (4) for the pseudo-atomic orbitals sum to a value somewhat greater than the total number of electrons in the system, and the plane-wave components compensate for this overcounting. Overcounting is more significant for the metallic system; in the case of bulk Pt, the magnitude of the plane-wave charge component is about 1.5e per atom, while for the Xe_2 dimer, as a result of the well-localized orbitals, it is only 0.02e per atom.

3. Calculated potentials

Potential energy curves, calculated using both the LDA and the GGA, are shown in figure 1 for Xe at the on-top, fcc-hollow and bridge sites. The hcp-hollow site is not shown as its potential is virtually indistinguishable from that of the fcc hollow. For comparison the Barker–Rettner potentials [16] (our parametrization of these is the same as that used by Kulginov *et al* [20]) for the $(\sqrt{3} \times \sqrt{3})$R30° structure are also shown. Although the Barker–Rettner curves cannot be regarded strictly as experimental results, the fact that they reproduce a wide range of experimental data means that they should be at least qualitatively correct.

The most striking feature of the calculated potentials is the weakness of the interaction obtained with the GGA-PBE form; it is clear that in this case the GGA results are in qualitative as well as quantitative disagreement with experiment. On the other hand, the LDA potentials agree reasonably well with the Barker–Rettner ones in the near-surface region, particularly for the hollow and bridge sites. The discrepancy observed in the longer-ranged, attractive part of the wells in figure 1 is expected as it is well known that the LDA fails to describe the asymptotic Van der Waals interaction [39].

Both LDA and GGA predict that the Xe–surface binding is strongest at the top site. The identification of the preferential adsorption site for Xe has been a subject of some controversy. On the basis of diffraction from the uniaxial incommensurate phase, Gottlieb [40] found the top site to be the most stable. This was supported both by Müller's LDA cluster calculation [14] and by Barker and Rettner [16], who found in construction of their empirical potential that a consistent fit with experiment could be obtained only by placing the Xe atom at the top site. However, this assignment was challenged by Zeppenfeld *et al* [41], and a later spin-polarized LEED experiment indicated a hollow-site adsorption [42] (although the determined adsorption height of 4.2 Å appears to be unphysically large). More recently the pendulum has swung back towards the top site, with Bruch *et al* [43] showing that this is consistent with their high-resolution He-atom scattering data, and a new LEED study favouring top-site adsorption with an adsorption height of 3.4 Å [44]. Although top-site adsorption might at first sight seem unlikely, there is experimental evidence that this is indeed the case for several Xe–metal systems (see [44, 45], and references therein).

Table 2 shows the well depth, equilibrium adsorption height and vibrational energy (estimated using the harmonic approximation) for the on-top site, calculated using a range of schemes. In each case the lattice constant of the slab is that given in table 1. The results obtained using an LDA cluster method and by experiment are also shown. The weakness of the interaction obtained with the GGA-PBE form is again apparent here, with a well depth of around

Table 2. The calculated well depth, V_0, equilibrium height, Z_0, and vibrational energy, E_v, for Xe atoms adsorbed on the Pt(111) surface at the on-top site.

	V_0 (meV)	Z_0 (Å)	E_v (meV)
LDA	332	3.11	5.6
LDA–NLCC	329	3.11	5.6
PBE	41	3.80	2.0
PBE–NLCC	39	3.79	2.0
LDA cluster[a]	307	3.00	8.5
Experiment	286[b]	3.4[c]	3.7[d]

[a] Reference [14].
[b] Reference [35].
[c] Reference [44].
[d] Reference [46].

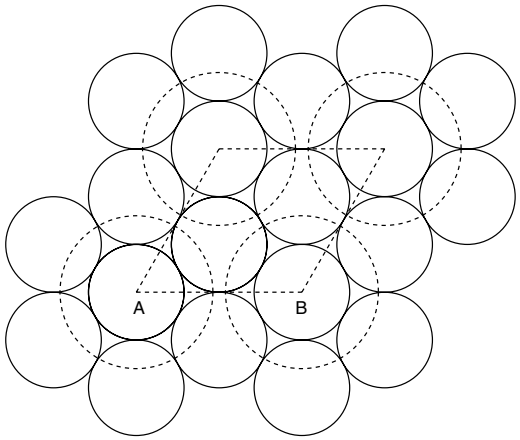

(a)

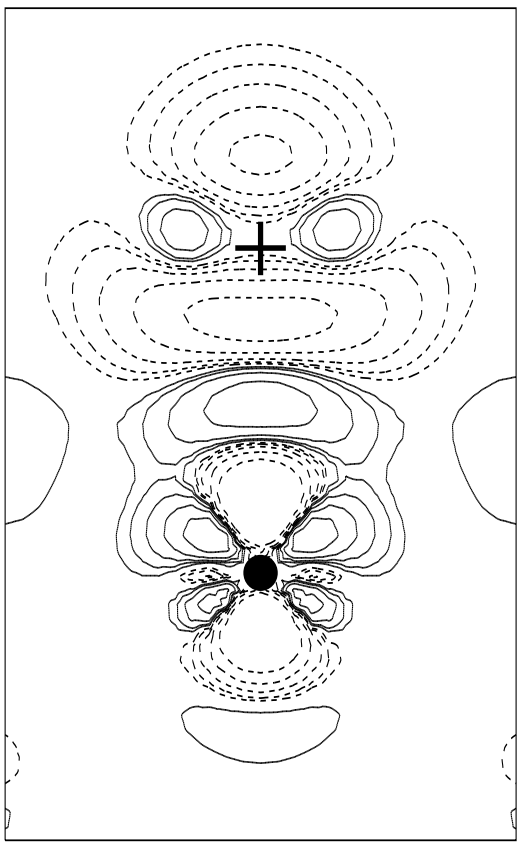

(b)

Figure 2. (a) Adsorption of xenon on Pt(111). Xe atoms are represented by dashed circles and Pt atoms in the first layer by full circles. The ($\sqrt{3} \times \sqrt{3}$)R30° cell is shown. (b) The charge-density difference induced by the adsorption of Xe atoms at the on-top site. Positives values are shown by solid lines and negative values with dashed lines. The contour lines represent densities given by $\pm 2^n \times 10^{-3}$ e Å^{-3}, $n = 1, \ldots, 5$. The positions of Xe and Pt atoms are shown by the cross and bullet symbols respectively.

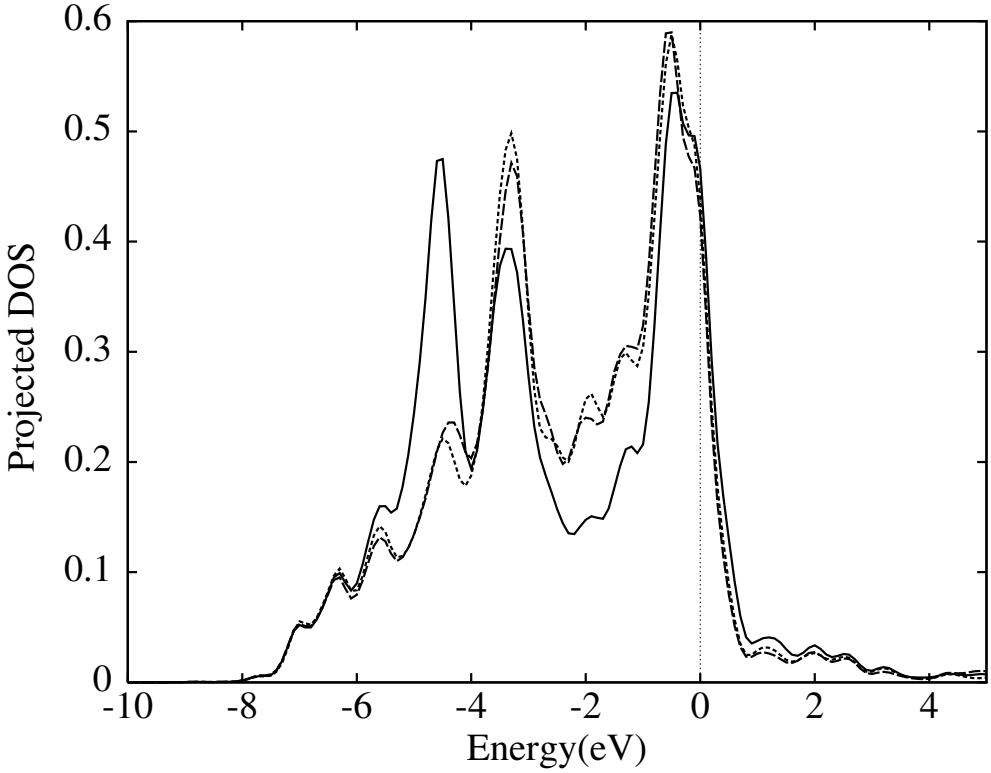

(a)

Figure 3. (a) The local density of states projected onto the d_{z^2} orbital of selected Pt atoms; the Pt atom directly below the Xe atom is represented by a solid line, the inequivalent Pt atom in the top layer is represented by a dashed line and a Pt atom in the bottom layer is represented by a dotted line. (b) The local density of states projected onto Xe orbitals. 5s, 5p and 5d are represented by solid, dashed and dotted lines respectively. The inset shows detail near the Fermi level.

40 meV. In contrast, the LDA gives a value of around 330 meV which is in reasonably good agreement with the most recent experimental estimate of 286 meV [35]. The equilibrium LDA adsorption height of 3.11 Å is also in fairly good agreement with Barker and Rettner's [16] value of 3.35 Å and the recent LEED measurement of 3.4 Å [44]. However, there is a considerable discrepancy in the vibrational energy for both LDA and the GGA-PBE form. The overall picture that emerges shows that the GGA predicts far too weak an interaction while the LDA, although closer to experiment, predicts a small overbinding. Finally, table 2 shows that there is no significant variation in the interaction potential when non-linear core corrections are taken into account.

The LDA well depths for the hcp-hollow, fcc-hollow and bridge sites are calculated to be 292 meV, 287 meV and 299 meV respectively, which should be compared to a value of 332 meV for the top site. The diffusion barrier is therefore predicted to be of the order of 35 meV (the equivalent GGA-PBE value is only 5 meV). This is similar to Barker and Rettner's value of 24 meV, and to the experimental estimates of 30 meV given by Kern *et al* [13] and 31 meV given by Horch *et al* [47]. However, a more recent experimental determination using quasielastic helium-atom scattering at low Xe coverage puts an upper limit on the diffusion barrier of 9.6 meV [48], indicating that there remains some uncertainty regarding this quantity.

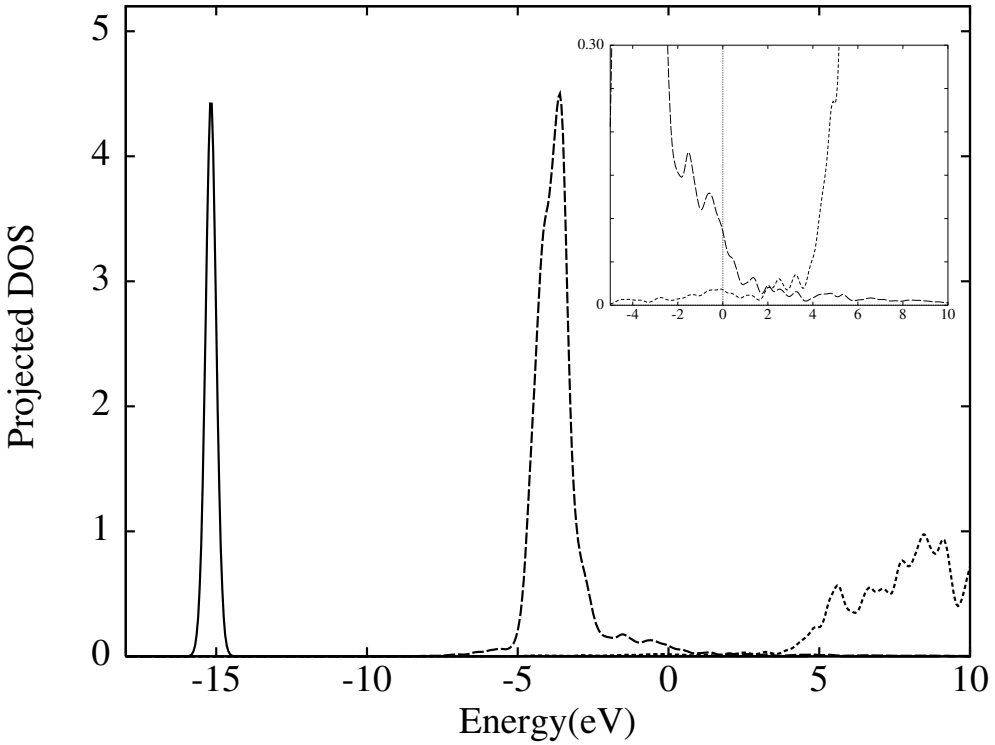

(b)

Figure 3. (Continued)

4. Binding mechanism

We now turn to an analysis of the binding mechanism for Xe on Pt(111). All the results below refer to LDA calculations at the on-top site and at the calculated equilibrium adsorption height. Figure 2(a) is a plan view of the ($\sqrt{3}\times\sqrt{3}$)R30° Xe/Pt(111) structure, and figure 2(b) displays a slice along the line AB of the charge-density difference $\rho(\text{slab+Xe}) - \rho(\text{slab}) - \rho(\text{Xe})$ induced by the adsorption of Xe atoms. There is a considerable reorganization of charge around both the Xe atom and the Pt surface atoms, demonstrating a significant element of chemisorption in this system. A dipole layer is created at the surface which induces a work-function change of $\Delta\Phi = -1.3$ eV, a value which is significantly different from -0.6 eV, as obtained by Cassuto and Erhardt using angle-resolved photoemission [49]. A considerable part of this discrepancy arises from the LDA overbinding apparent in table 2. If the work-function change is recalculated at the experimental adsorption height of 3.4 Å rather than at 3.11 Å, we obtain $\Delta\Phi = -0.9$ eV, which is closer to the experimental value.

To investigate the charge redistribution further we have calculated the total charge associated with particular orbitals, as defined in (4). Table 3 shows the change upon Xe adsorption in the integrated charge Q^i in the Xe orbitals and for the orbitals of the Pt atom directly below the adsorbed Xe. These orbitals are singled out because they show by far the largest changes. The Xe atom transfers approximately $0.05e$ to the Pt surface. However, there is also an internal reorganization within the Xe atom, consistent with the bonding charge density shown in figure 2(b), with a small occupation of 5d orbitals at the expense of the $5p_z$

Table 3. The change of the charge Q^i upon Xe adsorption at the on-top site for Xe and Pt orbitals. For Xe and Pt we refer to the 5s, 5p, 5d and 6s, 6p, 5d orbitals respectively. The Pt atom is directly below the adsorbed Xe. The total represents the net change over the atom.

Atom	s	p_x	p_y	p_z	d_{xy}	d_{yz}	d_{zx}	$d_{x^2-y^2}$	d_{z^2}	Total
Xe	+0.001	+0.003	+0.002	−0.091	+0.002	+0.012	+0.011	+0.001	+0.018	−0.041
Pt	−0.026	+0.013	+0.010	+0.064	+0.008	+0.014	+0.011	+0.009	−0.054	+0.049

state. It is interesting to note that the equivalent change in the charge associated with the low-energy plane-wave components in (1) is $-0.021e$. This is significant, because the adsorption of Xe on metal surfaces has frequently been discussed in terms of an interaction with the Xe 6s resonance (e.g. [18, 45, 50]). Because the 6s orbital is not included explicitly in our basis, we would expect its effects to be observed in the low-energy plane-wave component. The fact that the change in the plane-wave occupancy is negative implies that the plane waves contribute less in the combined adsorption system than in the component systems. Although one has to be careful not to over-interpret these small occupancy changes, our results indicate that it is the 5d resonance, rather than the 6s resonance, which has the most significant effect in the binding.

This picture is supported by the projected densities of states, as defined by (3). Figure 3(a) shows the density of states projected onto the d_{z^2} orbital of three Pt atoms. A comparison is made between the two inequivalent Pt atoms in the top layer of the slab (see figure 2(a)), and an atom in the bottom layer, which is essentially unaffected by Xe adsorption. The adsorption of an Xe atom is seen to make little difference to the Pt atom in the top layer further away from the adsorbate. However, for the Pt atom directly below the Xe atom, there is a distinct feature around 4.5 eV below the Fermi energy, which is associated with the interaction with the Xe 5p orbitals (mainly $5p_z$). This interaction also causes a broadening of the 5p states of the Xe atom, as shown in figure 3(b). A weak mixing of the 5p and 5d states of Xe is observed around the Fermi level (inset to figure 3(b)) which is consistent with the occupancy changes shown in table 3 and the bonding charge density shown in figure 2(b). The equivalent plot for the low-energy plane-wave component shows no obvious feature around the Fermi level, again indicating that the 6s resonance plays little part in the binding.

5. Conclusions

First-principles calculations of the interaction potential for Xe atoms on the Pt(111) surface have been presented. Neither LDA nor GGA-PBE potentials are in excellent agreement with the experimentally derived potential of Barker and Rettner [16] but the LDA potential is considerably closer. This is in contrast with the observation that the GGA usually gives substantially better adsorbate binding energies than the LDA. It is probably accidental that the LDA gives better agreement with experiment in this case, and our results should not be taken to imply that the general improvement in chemical binding energies provided by the GGA is invalid. However, they do show that a thoughtless application of DFT methods in less-common situations, like rare-gas interactions, can lead to incorrect conclusions and that a careful benchmarking with respect to experiment is vital. Although the LDA potential is closer to experiment, there are still significant errors in the well depth and adsorption height, and this overbinding is reflected in a substantial overestimation of the work-function change. The long-ranged part of the LDA potential, as expected, also shows a considerable deviation from experiment. The binding mechanism of the Xe/Pt(111) system has been analysed via

the density of states projected onto the atomic orbital and plane-wave basis functions of our mixed-basis method. A significant element of chemisorption is found, with the interaction with the Xe 5d resonance appearing to have the greatest effect in the binding.

Acknowledgments

AEB acknowledges support for this work from Universidad de Oriente and Consejo Nacional de Investigaciones Científicas y Tecnológicas (CONICIT) of Venezuela. We thank Mats Persson for providing the data for the Barker and Rettner potentials shown in figure 1.

References

[1] Farias D and Reider K-H 1998 *Rep. Prog. Phys.* **61** 1575
[2] Bird D M and Gravil P A 1997 *Surf. Sci.* **377–379** 555
[3] Hammer B and Nørskov J K 1997 *Chemisorption and Reactivity on Supported Clusters and Thin Films* ed R M Lambert and G Pacchioni (Dordrecht: Kluwer) pp 285–351
[4] Patton D C, Porezag D V and Pederson M R 1997 *Phys. Rev.* B **55** 7454
[5] Hammer B, Hansen L B and Nørskov J K 1999 *Phys. Rev.* B **59** 7413
[6] Perdew J P, Kurth S, Zupan A and Blaha P 1999 *Phys. Rev. Lett.* **82** 2544
[7] Zhang Y, Pan W and Yang W 1997 *J. Chem. Phys.* **107** 7921
[8] Patton D C and Pederson M R 1997 *Phys. Rev.* A **56** 2495
[9] Petersen M, Wilke S, Ruggerone P, Kohler B and Scheffler M 1996 *Phys. Rev. Lett.* **76** 995
[10] Trioni M I, Marcotulio S, Santoro G, Bortolani V, Palumbo G and Brivio G P 1998 *Phys. Rev.* B **58** 11 043
[11] Hult E, Rydberg H, Lundqvist B I and Langreth D C 1999 *Phys. Rev.* B **59** 4708
[12] Lang N D 1981 *Phys. Rev. Lett.* **46** 842
[13] Kern K, David R, Zeppenfeld P and Comsa G 1988 *Surf. Sci.* **195** 353
[14] Müller J E 1990 *Phys. Rev. Lett.* **65** 3021
[15] Weiss P S and Eigler D M 1992 *Phys. Rev. Lett.* **69** 2240
[16] Barker J A and Rettner C T 1992 *J. Chem. Phys.* **97** 5844
[17] Zeppenfeld P, Horch S and Comsa G 1994 *Phys. Rev. Lett.* **73** 1259
[18] Buldum A and Ciraci S 1996 *Phys. Rev.* B **54** 2175
[19] Weaver J F, Stinnett J A and Madix R J 1997 *Surf. Sci.* **391** 150
[20] Kulginov D, Persson M and Rettner C T 1997 *J. Chem. Phys.* **106** 3370
[21] Gülseren O, Bird D M and Humphreys S E 1998 *Surf. Sci.* **402–404** 827
[22] Kerker G P 1981 *Phys. Rev.* B **23** 3082
[23] Johnson D D 1988 *Phys. Rev.* B **38** 12 807
[24] Kresse G and Furthmüller J 1996 *Comput. Mater. Sci.* **6** 15
[25] Troullier N and Martins J L 1991 *Phys. Rev.* B **43** 1993
[26] Kleinman L and Bylander D M 1982 *Phys. Rev. Lett.* **48** 1425
[27] Bachelet G B, Hamann D R and Schlüter M 1982 *Phys. Rev.* B **26** 4199
[28] Ceperley D M and Alder B J 1980 *Phys. Rev. Lett.* **45** 566
[29] Perdew J P, Burke K and Ernzerhof M 1996 *Phys. Rev. Lett.* **77** 3865
[30] Perdew J P and Wang Y 1992 *Phys. Rev.* B **45** 13 244
[31] Fuchs M, Bockstedte M, Pehlke E and Scheffler M 1998 *Phys. Rev.* B **57** 2134
[32] Ozoling V and Körling M 1993 *Phys. Rev.* B **48** 18 304
[33] Barker J A, Watts R D, Lee J K, Schafer T P and Lee Y 1974 *J. Chem. Phys.* **61** 3081
[34] Khein A, Singh D J and Umrigar C J 1995 *Phys. Rev.* B **51** 4105
[35] Widdra W, Trischberger P, Friess W, Menzel D, Payne S H and Kreuzer H J 1998 *Phys. Rev.* B **57** 4111
[36] Sánchez-Portal D, Artacho E and Soler J M 1996 *J. Phys.: Condens. Matter.* **8** 3859
[37] Börnsen N, Meyer B, Grotheer O and Fähnle M 1999 *J. Phys.: Condens. Matter* **11** L287
[38] Mulliken R S 1955 *J. Chem. Phys.* **23** 1833
[39] Lang N D and Nørskov J K 1983 *Phys. Rev.* B **27** 4612
[40] Gottlieb J M 1990 *Phys. Rev.* B **42** 5377
[41] Zeppenfeld P, Comsa G and Barker J 1992 *Phys. Rev.* B **46** 8806
[42] Potthoff M, Hilgers G, Müller N, Heinzmann U, Haunert L, Braun J and Borstel G 1995 *Surf. Sci.* **322** 193
[43] Bruch L W, Graham A P and Toennies J P 1998 *Mol. Phys.* **95** 579

[44] Seyller Th, Caragiu M, Diehl R D, Kaukasoina P and Lindroos M 1999 *Phys. Rev.* B **60** 11 084
[45] Narloch B and Menzel D 1997 *Chem. Phys. Lett.* **270** 163
[46] Hall B, Mills D L, Zeppenfeld P, Kern K, Becher U and Comsa G 1989 *Phys. Rev.* B **40** 6326
[47] Horch S, Zeppenfeld P and Comsa G 1995 *Surf. Sci.* **311–333** 908
[48] Ellis J, Graham A P and Toennies J P 1999 *Phys. Rev. Lett.* **82** 5072
[49] Cassuto A and Erhardt J J 1988 *J. Physique* **49** 1753
[50] Eigler D M, Weiss P S, Schweitzer E K and Lang N D 1991 *Phys. Rev. Lett.* **66** 1189